Solar Energy, Vol. 19, pp. 389–393. Pergamon Press 1977. Printed in Great Britain

Vol. 19, No. 4, 1977

TECHNICAL NOTE

The effect of dropwise condensation on glass solar properties

C. K. HSIEH and ANIL K. RAJVANSHI

Dept. of Mechanical Engineering, University of Florida, Gainesville, FA 32611, U.S.A.

(*Received* 11 *December* 1975)

INTRODUCTION

The change of heat transfer characteristics of surfaces covered with water condensation has been a subject of intense research only insofar as it is related to heat convection. Not thoroughly studied is the change of surface radiative characteristics due to presence of such condensate. In fact, in the flat plate solar collector, especially in the solar distillator, dropwise condensation on glass surface often occurs and can be a dominating factor affecting the performance of the device.

There are two factors which make the study of surface radiative characteristics of dropwise condensation less-than-trivial. The first is the rapid variation of water absorption coefficient with wavelength. With the water droplet varying in size in practice, its transmission and reflection cannot be predicted with reasoning. The second complication is the fact that, when radiation enters into the water droplet and crosses the water-air interface, because of the smaller refractive index occuring at the air side, total reflection will take place for rays of large incident angles. These rays will also experience longer path lengths of traveling, thereby attenuating more energy. As a result, the multireflections in the water droplet cannot be neglected and this complicates the formulation.

It is the purpose of this paper to evaluate the thermal radiative properties of glass covered with dropwise condensation on one side of the surface. Property values presented in this paper include normal spectral transmittance and reflectance for the condensate covered glass surface and the resulting bulk glass spectral properties. Finally these spectral properties are integrated to yield the total properties in the solar system.

FORMULATION

The configuration of a water droplet adhered to a glass surface depends on, among others, the contamination on the glass surface. It is not unreasonable to assume the water droplet being a half sphere and the incident ray normal to the glass-water interface. For simplicity reasons, diffraction, polarization and interference effects are negligible. The glass-water and water-air interfaces are ideal to the extent that the electromagnetic theory is useful in predicting the radiative properties.

Based on the model depicted in Fig. 1 the energy incident on the circular area at the glass-water interface can be expressed as

$$dQ_i = I_\lambda \pi r_0^2 \, d\omega \, d\lambda \, dt. \tag{1}$$

The energy transmitted through the water droplet and emerged from the water-air interface is

$$dQ_t = I_\lambda \, d\omega \, d\lambda \, dt \int_0^{r_0} \tau_{G-W,0}\tau_{W-A,\delta} \exp(-\kappa_{\lambda,W}\overline{AC}) 2\pi r \, dr \tag{2}$$

where $\tau_{G-W,0}$ represents transmittance at the glass-water interface for radiation incident in normal direction. From the electromagnetic theory, this transmittance is related to the refractive indices of the media as

$$\tau_{G-W,0} = 4n_g n_w/(n_g + n_w)^2. \tag{3}$$

Likewise, the transmittance at the water-air interface for incidence at δ angle from normal can be expressed as the Fresnel's equation

$$\tau_{W-A,\delta} = 1 - 0.5[\sin^2(\delta - \nu)/\sin^2(\delta + \nu)] \times \{1 + [\cos^2(\delta + \nu)/\cos^2(\delta - \nu)]\}. \tag{4}$$

From geometry, the path length of attenuation for absorption

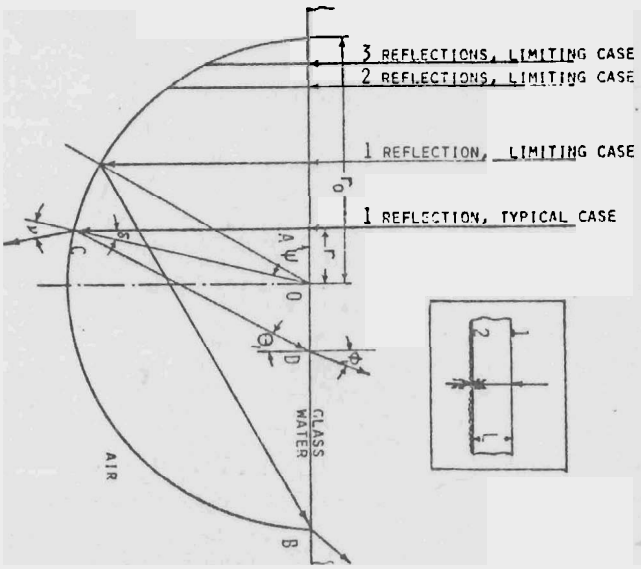

Fig. 1. Reflection pattern in a water droplet.

coefficient $\kappa_{\lambda,w}$ can be related to r and r_0 as

$$\overline{AC} = (r_0^2 - r^2)^{1/2}. \quad (5)$$

The upper limit of integration is r_c, given as

$$r_c = (r_0/n_w) \quad (6)$$

which is derived on the basis of the fact that, when the incident radiation reaches a critical angle, total reflection takes place. Obviously, Snell's law has been used here in determining this angle. This same law is also used to find ν in eqn (4).

The energy reflected from the glass-water interface will experience a first reflection from this interface. This energy is quite small due to the closeness of the n_g and n_w values. Calculations show 99 per cent of the energy is transmitted through this interface and enters into the water droplet in the solar spectrum. Depending on the location of the incident ray measured away from the center of the droplet, the incident ray can experience a single reflection, or multiple reflections at the water-air interface. A typical one-reflection case and the one-reflection, limiting case are illustrated in Fig. 1 where the latter is determined by geometrical ray tracing in the figure. For this limiting case, the reflected ray impinges on the glass-water-air triple point B. A further increase in r for the incident ray will result in double reflections easily visualized from geometry.

Following the same approach as previously used in deriving the transmitted energy, the reflected energy can be expressed as

$$\begin{aligned} dQ_r = I_\lambda\, d\omega\, d\lambda\, dt \Big\{ & [(n_g - n_w)/(n_g + n_w)]^2 \pi r_0^2 \\ & + \int_0^{0.5 r_0} \tau_{G-W,0} \tau_{W-G,\theta_1} \rho_{W-A,\beta} \\ & \times \exp[-\kappa_{\lambda,w}(\overline{PL})_1] 2\pi r\, dr + \int_{0.5 r_0}^{r_c} \tau_{G-W,0} \tau_{W-G,\theta_2} \rho^2_{W-A,\beta} \\ & \times \exp[-\kappa_{\lambda,w}(\overline{PL})_2] 2\pi r\, dr + \int_{r_c}^{r_0 \cos(\pi/5)} \tau_{G-W,0} \tau_{W-G,\theta_2} \\ & \times \exp[-\kappa_{\lambda,w}(\overline{PL})_2] 2\pi r\, dr + \sum_{n=3}^{\infty} \int_{r_0 \cos[\pi/(2n+1)]}^{r_0 \cos[\pi/(2n-1)]} \\ & \times \tau_{G-W,0} \tau_{W-G,\theta_n} \exp[-\kappa_{\lambda,w}(\overline{PL})_n] 2\pi r\, dr \Big\}. \end{aligned} \quad (7)$$

Where the first term in the braces represent the first reflection from the glass-water interface; the second term, the contribution of the energy entering into the water droplet, attenuated by the water medium, and reemerged from the glass-water interface. The attenuation path length $(\overline{PL})_1$ equals $(\overline{AC} + \overline{CD})$ for the single reflection case. For double reflections, the integral has to be split into two parts. For rays impinging on the circular ring from r_c to $r_0 \cos(\pi/5)$, total reflection occurs at the water-air interface, thereby enabling the reflectance term to be eliminated from the integral. For higher order reflections, the contribution is expressed in a summation. The path lengths for attenuation in the water droplet can be expressed in a general form as

$$(PL)_m = (2m-1)(r_0^2 - r^2)^{1/2} - r_0[\sin(2m-1)\psi]/\cos 2m\psi. \quad (8)$$

Where m denotes the number of reflections at the water-air interface,

$$\psi = \cos^{-1}(r/r_0). \quad (9)$$

The incident angle at the glass-water interface can also be expressed in a general equation.

$$\theta_m = \pi - 2m \cos^{-1}(r/r_0). \quad (10)$$

With the same m defined previously, τ_{W-G,θ_m} can again be expressed as the Fresnel's equation, eqn (4), with the Snell's law again used to establish the relation between incident and refracted angles, θ_m and ϕ_m.

The normal spectral transmittance and reflectance for the condensate covered glass surface can now be calculated by dividing eqn (2) by (1) for the transmittance and eqn (7) by (1) for the reflectance. Of course for those areas on the glass surface where no droplets are formed, surface property equations for glass-air interface can be used.

It should be noted that, because of the presence of the spherical water droplet, the energy reflected from the condensate covered glass surface becomes somewhat diffuse. In fact, eqn (10) can be used to calculate the incident angle at the glass-water interface. For all the cases considered in Fig. 1, this incident angle never exceeds 60° (see Table 1). More specifically, only for incident rays impinging in the circular ring from 0.309 to 0.5 r_0, the reflected rays will incident at θ_1 ranging from 36 to 60° at the glass-water interface. In fact, the great majority of the reflected energy is incident at θ angles less than 36°. The larger n_g values further reduce the refracted angle in the glass medium to less than 30°. Hence the reflected energy from the glass-water interface retains predominantly in a normal direction pattern which enables one to use[1]

$$\tau_B = \tau_1 \tau_2 \exp(-\kappa_{\lambda,g} L)[1 - \rho_1 \rho_2 \exp(-2\kappa_{\lambda,g} L)]^{-1} \quad (11)$$

$$\rho_B = \rho_1 + \rho_2 \tau_1^2 \exp(-2\kappa_{\lambda,g} L)][1 - \rho_1 \rho_2 \exp(-2\kappa_{\lambda,g} L)]^{-1} \quad (12)$$

to find the bulk glass properties for a glass plate of thickness L. Here in eqns (11) and (12) subscripts 1 and 2 for surface properties refer to bare surface 1 and condensate covered surface 2, respectively, with surface 1 facing toward the incoming radiation, see inset of Fig. 1. Since both surface and bulk properties are functions of the refractive indices and absorption coefficients which are, in turn, functions of wavelengths, they are spectral properties. An integration using weighted ordinates approach[2] has to be used to yield total properties in the solar spectrum.

To further amplify the utility of this study, a more realistic model is considered which has a fraction of the glass surface area covered with dropwise condensation. For this model, the glass properties can be changed to

$$\tau = C_\tau \tau_{clean} \quad (13)$$

and similarly

$$\rho = C_\rho \rho_{clean}. \quad (14)$$

Where both C_τ and C_ρ are correction factors established on the basis of clean glass properties τ_{clean} and ρ_{clean}. These correction factors can be derived and written as, for transmittance,

$$C_\tau = (1 - F) + F(\tau_{water\ covered}/\tau_{clean\ glass}). \quad (15)$$

Where F represents the fraction of the glass surface area covered with water droplets.

RESULTS AND DISCUSSION

In this paper, the refractive index and absorption coefficient values for glass were taken from[1, 3]. The data for water were

Table 1. Incident angles (θ_m) at the glass-water interface

Number of reflections at the water-air interface	Ranges of incidence angles (θ_m) at the glass-water interface
1	$0 - \frac{\pi}{3}$
2	$\frac{\pi}{3} - \frac{\pi}{5}$
3	$\frac{\pi}{5} - \frac{\pi}{7}$
4	$\frac{\pi}{7} - \frac{\pi}{9}$
5	$\frac{\pi}{9} - \frac{\pi}{11}$

taken from [4]. The absorption coefficient of water is highly spectral dependent, a plot of this absorption coefficient is thus given in Fig. 2 to facilitate later discussion with regard to the change of surface properties. Equations used in the calculation were programmed in an IBM 370 computer to generate data relevant to the study.

The surface transmittance and reflectance curves for condensate covered glass surface are shown in Figs. 3 and 4 where the

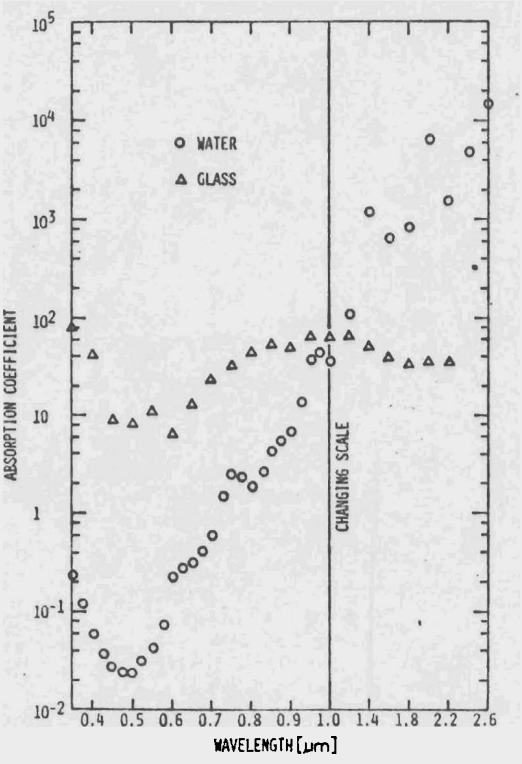

Fig. 2. Absorption coefficient of water and glass.

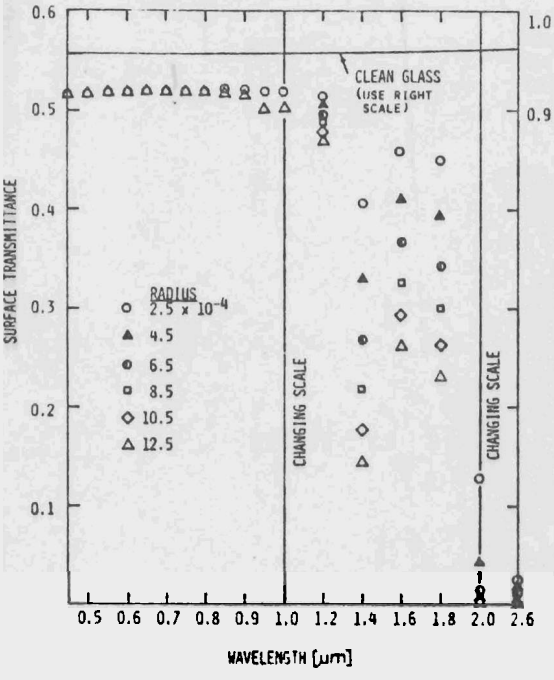

Fig. 3. Surface spectral transmittance for condensate covered glass surface.

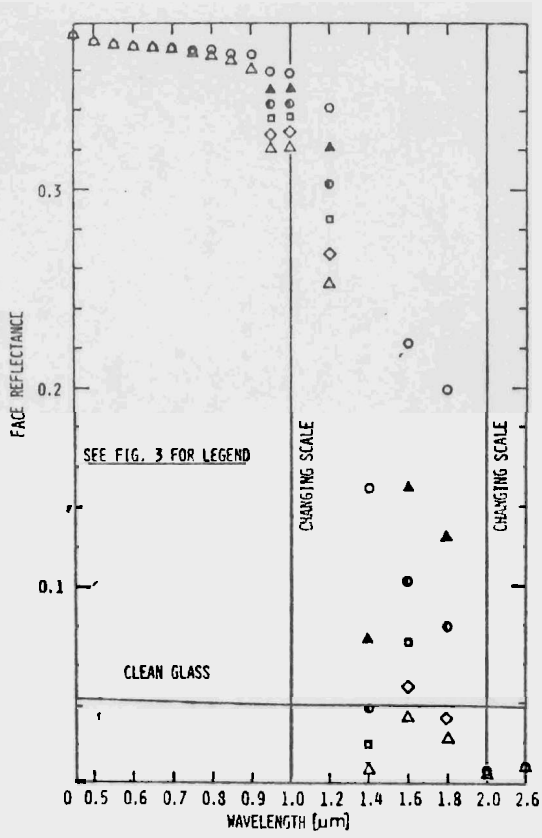

Fig. 4. Surface spectral reflectance for condensate covered glass surface.

radius of the water droplet was used as a parameter. The behavior of the glass surface was contrasted with that of a clean surface curve which typically demonstrates high transmittance and low reflectance behavior. As seen in the figures, below 0.9 μ, the surface transmittance and reflectance values are independent of the wavelength and the size of the water droplet. This could be ascribed to the relatively low absorption coefficient of water at these wavelengths. There is, nevertheless, a considerable increase in surface reflectance, 9 times over that for clean surface as well as a drop in transmittance (46 per cent) for the water covered surface. Beyond 0.9 μ, both transmittance and reflectance values decline, also the size of the water droplet comes into play. As expected, the bigger the water droplet, the more severe is the energy attenuation, thereby diminishing both transmittance and reflectance values. Such a trend is seen to be more pronounced at 1.4 and 2 μ, coincident with the rapid increase in the water absorption coefficient demonstrated in Fig. 2. A careful examination of the spacing between data points at a given wavelength further substantiates that both surface transmittance and reflectance drop exponentially with increase of the size of the water droplet as is in conformity with what one might surmise by reasoning. At 2.6 μ, the water becomes so absorptive that the surface properties becomes, once again, insensitive to the droplet size. Both transmittance and reflectance values drop below 2 per cent. As the water absorption coefficient will further increase toward longer wavelengths, this low reflectance and transmittance behavior is expected to persist in the far infrared.

The calculated surface properties given above were subsequently applied as one surface of a glass plate and used to evaluate the bulk glass properties. A Libbey–Owens–Ford single strength sheet glass of 0.2286 cm thickness was selected as a case study and data plotted as shown in Figs. 5 and 6. Both bulk transmittance and reflectance curves are seen to drop at about 0.65 μ which can be attributed this time to the increase in the glass absorption in the same spectrum, also see Fig. 2. Again the decrease in glass transmittance and increase in reflectance trends

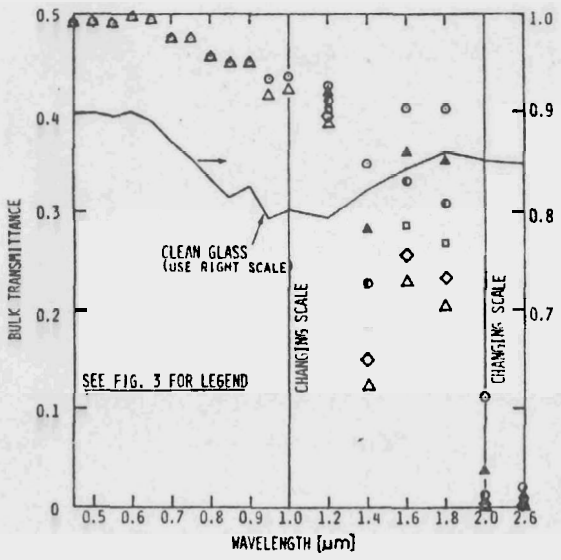

Fig. 5. Bulk glass spectral transmittance curves.

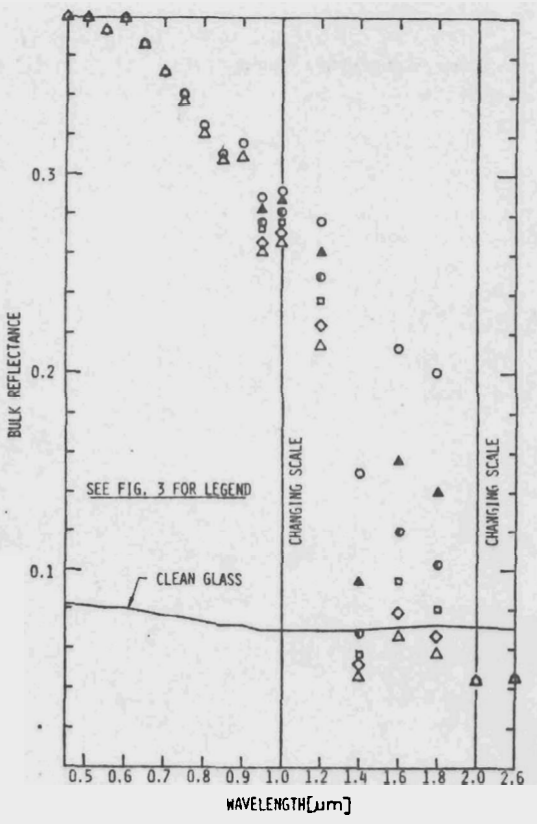

Fig. 6. Bulk glass spectral reflectance curves.

are significant. In the visible part of the spectrum, the bulk transmittance of a water covered glass plate reaches only 55 per cent of that for a clean glass while the reflectance is about 4.8 times higher. Much of the trend observed in the previous paragraph is also valid here, with the same course of transmittance and reflectance variations following that of the transmittance curve for a clean glass at shortwavelengths as shown in Fig. 5.

The spectral properties presented in Figs. 3-6 were subsequently integrated over the solar spectrum to yield total properties with the result presented in Fig. 7. As the energy contained below 0.9 μ constitutes about 71 per cent of the total energy in the solar spectrum, it is not surprising that both surface and bulk properties of water covered glass is quite insensitive to the size of the water droplet. It should be noted that a clean glass surface has a surface solar transmittance of 0.958 and reflectance of 0.042. A clean glass plate has bulk transmittance 0.853 and reflectance of 0.075. Thus with dropwise condensation occuring on one surface, the bulk solar transmittance of glass drops about 48 per cent while reflectance increases 4.2 folds for the size of the water droplet studied. The presence of dropwise condensation has thus proved to present a serious problem reducing the actual energy that can be received in a solar energy device.

Since the glass properties studied here have shown to be relatively insensitive to the size of the water droplet, it makes sense to stride one step further to develop correction factor curves for a more realistic case with only a fraction of the total glass surface covered with dropwise condensation. Both correction factors for surface properties and bulk properties have been calculated and plotted as shown in Fig. 8. Equations (13) and (14) describe how these correction factors are used to modify

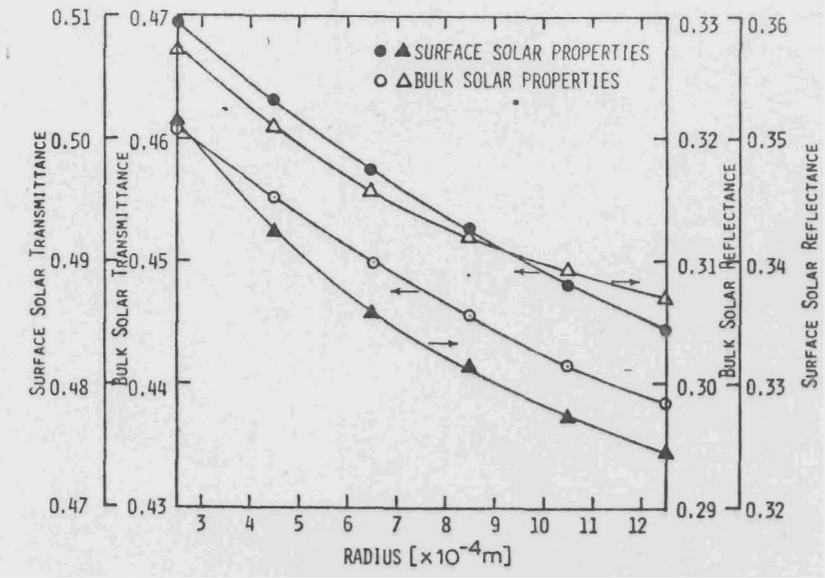

Fig. 7. Solar reflectance and transmittance curves.

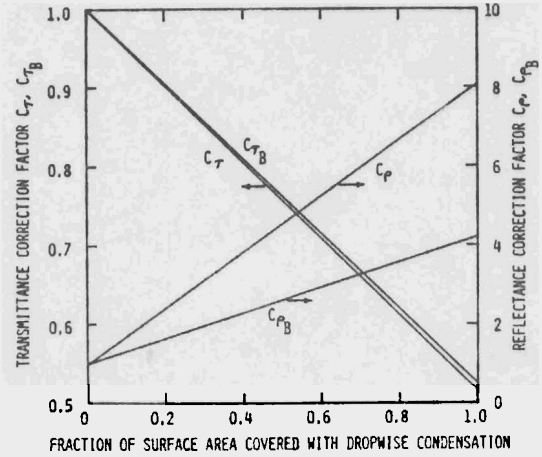

Fig. 8. Correction factor curves for overall surface.

properties. With the small change of glass properties between single and double strength glasses[1], the correction curves C_{τ_B} and C_{ρ_B} herein developed on the basis of a single strength glass, are also valid in practice for a double strength glass plate.

NOMENCLATURE

C_τ correction factor for transmittance
C_ρ correction factor for reflectance
I_λ spectral intensity of radiation
L thickness of glass
m no. of reflections at the water-air interface
n_g refractive index of glass
n_w refractive index of water
Q_i energy incident on the surface
r_0 radius of the droplet
r_c critical radius as given by eqn (6)
t time

Greek symbols

δ angle of incidence at water-air interface
θ_m incident angle at glass-water interface in the most general form
$\kappa_{\lambda,w}$ spectral absorption coefficient of water
$\kappa_{\lambda,g}$ spectral absorption coefficient of glass
λ wavelength
ν angle of refraction at water-air interface
$\rho_{i-j,k}$ reflectance at $i-j$ interface for the ray incident at an angle k
ρ_B bulk reflectivity
$\tau_{i-j,k}$ transmittance at $i-j$ interface for the ray incident at an angle k
τ_B bulk transmittance
ψ given by eqn (9)
ω solid angle

Subscripts

A
W water
1 bare surface
2 condensate covered surface

REFERENCES

1. C. K. Hsieh, *Study of Thermal Radiative Properties of Glass.* TRL Report, Thermal Radiation Laboratory, Department of Mechanical Engineering, University of Florida (1973).
2. ASTM Standard E 424–71, *Standard Method of Test for Solar Energy Transmittance and Reflectance (Terrestrial) of Sheet Materials.*
3. G. W. Cleek *et al.*, Refractive indices and transmittances of several optical glasses in the infrared. *J. Opt. Soc. Am.* 49 (11), 1090–1095 (1959).
4. G. M. Hale and R. Querry, Optical Constants of Water in the 200 nm to 200 μm Wavelength Region. *Appl. Opt.* 12 (3), 555–563 (1973).